MPI 632

Original Paper

Cerebrovascular Diseases

Cerebrovasc Dis 2003;16:158–165
DOI: 10.1159/000070596

Received: June 13, 2002
Accepted: October 9, 2002

Determination of Cerebrovascular Reactivity by Means of fMRI Signal Changes in Cerebral Microangiopathy: A Correlation with Morphological Abnormalities

Margret Hund-Georgiadis[a] Stefan Zysset[a] Shinji Naganawa[b]
David G. Norris[c] D. Yves von Cramon[a]

[a]Max Planck Institute of Cognitive Neuroscience, Leipzig, Germany; [b]Department of Radiology, Nagoya University School of Medicine, Nagoya, Japan; [c]FC Donders Centre for Cognitive Neuroimaging, Trigon, Nijmegen, The Netherlands

Key Words
Hyperventilation · Cerebrovascular reactivity · Functional magnetic resonance · Cerebral microangiopathy

Abstract
Background and Purpose: A reduced cerebrovascular reactivity (CR) is a risk factor of cerebrovascular disease. In this study, we implemented a protocol to assess CR by means of functional MRI (fMRI) using hyperventilation. ***Subjects and Methods:*** In 5 patients with cerebral microangiopathy (CM/lacunar infarction and white matter degeneration), 6 healthy elderly subjects (age-matched control), and 6 young healthy subjects, the CR in response to hyperventilation was evaluated by fMRI using gradient echo-planar Imaging. The percentage signal change normalized by end-tidal CO_2 value was measured in various brain regions. ***Results:*** All subjects performed hyperventilation well without adverse reaction and significant gross motion. Patients with CM showed significant qualitative and quantitative differences ($p < 0.05$) as compared to controls. The volume of gray matter showing significant CR was significantly reduced in patients: by 40% in comparison to the age-matched elderly control group and by 60% when compared with the young controls. The CR impairment was most pronounced in the frontal cortices with a drastically reduced magnitude of the magnetic resonance (MR) signal change in the patients (–0.62 ± 0.2% in patients versus –2.0 ± 0.36% in age-matched controls, $p < 0.0001$). A strong relation was evident between the fMRI-based CR reduction in patients with CM and the individual severity of structural MR abnormalities ($p = 0.002$). ***Conclusion:*** This study demonstrates that fMRI-based signal changes in response to hyperventilation reliably reflect cerebral vasoreactivity. The protocol is feasible in healthy young and elderly controls and patients with CM. Quantitative and qualitative assessment of the signal decrease in the T_2-weighted MR sequence and coregistration with individual anatomical data allow the generation of an individual cerebral vasoreactivity map. Future research will address the effect of CR reduction on neuropsychological parameters in patients with CM.

Introduction

Cerebral microangiopathy (CM) is a common neurological disease, with a prevalence of 3.8–6.7% in individuals older than 50 years [1]. Morphological white matter

KARGER
Fax + 41 61 306 12 34
E-Mail karger@karger.ch
www.karger.com

1015–9770/03/0162–0158$19.50/0

Accessible online at:
www.karger.com/ced

Margret Hund-Georgiadis
Max Planck Institute of Cognitive Neuroscience
Stephanstrasse 1a
D–04103 Leipzig (Germany)
Tel./Fax +49 341 9940 161, E-Mail hund@cns.mpg.de

abnormalities are the main magnetic resonance (MR) characteristics [2]. Structural damage to the deep white matter is due to a perfusion deficit caused by lipohyalinosis of cerebral arterioles, resulting in a variety of clinical symptoms, neuropsychological abnormalities and MRI characteristics [3, 4]. CM coincides with arterial hypertension and other vascular risk factors. Recently, a loss of cerebral autoregulation was described in patients with CM [5–7]. Impaired cerebrovascular reactivity (CR) could be responsible for further subcortical infarctions and thus progression of the disease.

Hypo- and hypercapnic challenges have been established as reliable alternatives to assess global CR, using various imaging techniques, mainly xenon-133 single photon emission tomography (SPECT) [8], positron emission tomography (PET) [9], transcranial Doppler sonography (TCD) [10, 11] and recently near infrared spectroscopy (NIRS) [12]. Functional MRI (fMRI) presents a new diagnostic tool to assess regional CR, with high spatial resolution [13–15]. Previous studies utilized a hyperventilation experiment in normal subjects at 1.5 [13, 14] and at 3 T [15]. However, the effects of aging and feasibility of fMRI have not been addressed in clinical studies to date, with the single exception of a study examining distressed infants [16]. Thus, no clinical protocol has yet been established for the application of fMRI for the evaluation of CR. fMRI represents a promising approach for several reasons: first, the procedure is noninvasive and repeatable. Second, in contrast to other techniques, it could offer a 3D cerebral vasoreactivity map that takes into account regional differences in vascular response. The fMRI-based vasoreactivity assessment employs the blood oxygenation level dependent (BOLD) contrast with deoxyhemoglobin as an endogenous intravascular contrast agent. Hyperventilation is associated with hypocapnia, which induces a constriction of small arterial vessels (mainly at the arteriole level) in healthy individuals. A decrease in cerebral blood flow ensues. Such a decrease without a concomitant decrease in cerebral metabolic rate of oxygen will lead to increased paramagnetic deoxyhemoglobin levels and thereby decreases in the T_2-weighted MRI signal intensities.

An fMRI protocol to measure hyperventilation-induced CR in patients with CM was established in the present study. We hypothesize that patients with CM show a smaller and spatially more heterogeneous MR signal decrease in response to hypocapnia in contrast to healthy controls. The applied fMRI methodology to assess CR was subsequently compared with established methods of CR assessment. Furthermore, the issue of age-related changes of cerebral autoregulation was addressed, based on two groups of healthy controls, differing by age. Changes in CR in the patient group examined were related to clinical and morphological MR data.

Subjects and Methods

Subjects

Six young healthy subjects (3 males and 3 females, aged 23–27 years, mean 24.8 years), 6 healthy elderly subjects without any history of neurological disorders (4 males and 2 females, aged 51–63 years, mean 57 years), and 5 patients with CM, who had previously been diagnosed on the basis of both clinical and anatomical T_2-weighted MRI (3 males and 2 females, aged 54–67 years, mean 61.8 years) were included in this pilot study.

The severity of structural abnormalities was rated according to an established MR rating scale [17]. Scores theoretically range from 0 to 21. Based on the MR score, the severity of CM was assessed as low (scores of less than 6 points), moderate (score between 6 and 12 points) and severe (score higher than 12 points). Based on this scaling, 3 patients suffered from severe and 2 from moderate CM. None of the patients showed cortical atrophy. Stenosis of extracranial and basal cerebral arteries was excluded by means of extracranial duplex and transcranial Doppler. No cortical infarction or intracerebral hemorrhage was diagnosed in any of the 5 patients. Clinical details of the enrolled patients, including the Scandinavian Stroke Scale [18], prevalence of relevant vascular risk factors (diabetes mellitus, hyperlipidemia and arterial hypertension), as well as MR severity scores are summarized in table 1. The diagnosis of diabetes mellitus was based on an oral glucose tolerance test. The grade of arterial hypertension was determined using the WHO classification. All subjects gave their written informed consent to participate in this study, which was approved by the local ethical committee.

MR Imaging

The experiment was performed using a 3-tesla whole-body scanner (Bruker Medical, Ettlingen, Germany). Sixteen axial slices (19.2 cm FOV, 64 × 64 matrix, 5 mm thickness, 1 mm spacing) parallel to the AC-PC plane covering the whole brain were acquired using an single shot, gradient recalled echo-planar imaging sequence (TR 2000 ms, TE 75 ms; 90° flip angle). Prior to functional MR mapping, 16 anatomical T_1-weighted MDEFT [19] images (256 by 256 matrix, TR 1300 ms, TE 10 ms) and 16 T_1-weighted echo-planar images (EPI) with geometrical parameters identical to those of the fMRI data were recorded.

Hyperventilation Experiment

After 4 min of normal breathing (baseline condition), all subjects were instructed to perform voluntary hyperventilation for 2 min (activation condition) by the operator. This 6-min block was repeated three times. The total scan time was 18 min per run. To control the effects of hyperventilation in each individual subject, the end-tidal CO_2 partial pressure ($EtCO_2$) was continuously monitored via a nasal cannula using the 'Maglife' capnometer (Bruker Medical, Ettlingen, Germany).

Data Analysis

The fMRI data were processed on an SGI Origin 2000 with the LIPSIA software [20]. This software package contains tools for pre-

Table 1. Clinical data and history of each patient

Demographic variables				SSC[a]	MRS[b]	Risk factor profile				
patient	age	gender	TSD[c] years			diabetes	obesity (BMI >29)	smoking	hyperlipid-emia	hypertension (duration)
1	66	m	3	50	7	Y	N	N	N	II (>7 years)
2	59	m	1	42	9	N	N	Y	N	II (>2 years)
3	54	f	<1	46	12	N	Y	N	Y	N
4	63	f	4	42	14	N	N	Y	Y	II (?)
5	67	m	3	46	16	N	Y	N	Y	I (>13 years)

[a] Scandinavian Stroke Score.

[b] MR score; scores theoretically range from 0 to 21. The severity of CM was assessed based on the MR score: low-degree CM was assessed with scores of less than 6 points, moderate severity was defined when the score ranged between 6 and 12 points, severe CM was declared, when scores were higher than 12 points.

[c] Time since onset of the disease.

processing, registration, statistical evaluation and visualization of fMRI data.

Functional data were corrected for motion using a matching metric based on linear correlation. To correct for the temporal offset between the slices acquired in one scan, a sinc-interpolation based on the Nyquist-Shannon theorem was applied. A spatial Gaussian filter with 5.65 mm FWHM was applied.

To align the functional data slices onto a 3D stereotactic coordinate reference system, a rigid linear registration with 6 d.f. (3 rotational, 3 translational) was performed. The rotational and translational parameters were acquired on the basis of the MDEFT and EPI-T1 slices to achieve an optimal match between these slices and the individual 3D reference data set, which was acquired for each subject during a previous scanning session. The 3D-MDEFT [21] volume data set (128 sagittal slices, 1.5 mm thickness, FOV 25.0 × 25.0 × 19.2 cm, data matrix of 256 × 256) was standardized to the Talairach stereotactic space [22]. The resulting rotational and translational parameters were normalized, i.e., transformed by linear scaling to a standard size and used to transform the functional slices by means of trilinear interpolation, so that the resulting functional slices were aligned with the stereotactic coordinate system.

The statistical evaluation of fMRI data was based on a least-squares estimation using the general linear model for serially autocorrelated observations [23–26]. The design matrix was generated utilizing a box-car function and a response delay of 6 s. The model equation, including observation data, design matrix and error term, was convolved with a Gaussian kernel with a dispersion of 4 s. The contrast between the different conditions was calculated using the t statistic. Subsequently, t values were transformed to z scores. As all the individual functional data sets were mapped to the same stereotactic reference space, a group analysis was subsequently performed. A Gaussian test was computed, indicating whether observed differences between conditions were significantly different from zero [27].

The signal time courses for six different and representative regions of interest (ROI) in all brain lobes were then extracted. The ROIs were located in the frontal (s. frontalis sup. and s. precentralis), parietal (s. intraparietalis), temporal (s. temporalis sup. and s. lingualis) occipital (calcarina) and cerebellar (lobus anterior/ fissura prima) cortex in both hemispheres. For each ROI, the signal of the center voxel and its 26 neighbors was averaged for the three repetitions and both hemispheres separately for the three study groups. The percent signal change was calculated for each time point against the time interval between 2 and 3 min of the resting state. Statistics of clinical data and group comparisons were conducted using computerized statistical software. Independent t tests were used to test differences between study groups. Normally distributed data were expressed as mean ± standard deviation. A p value <0.05 was considered statistically significant. To assess the relationship between clinical data and the spatial distribution and extent of MR signal changes, a bivariate correlation analysis using the Pearson coefficient was performed.

Results

Hyperventilation Effects

All subjects performed hyperventilation well, without any adverse side reactions or detectable gross head motion. The individual $EtCO_2$ values were decreased at least by 10 mm Hg in all subjects, which was the cutoff in each individual to define successful hyperventilation. The mean $EtCO_2$ change was 19.9 ± 4.6 mm Hg in young healthy subjects, 17.8 ± 5.4 mm Hg in elderly healthy subjects, and 19.9 ± 5.0 mm Hg in patients with CM. The effects of hyperventilation did not differ significantly between groups (all $p > 0.05$, t test for unpaired samples).

MR Signal Changes

Hyperventilation was associated with significant decreases in the BOLD signal in all cortical regions. The hyperventilation-induced MR signal changes showed sig-

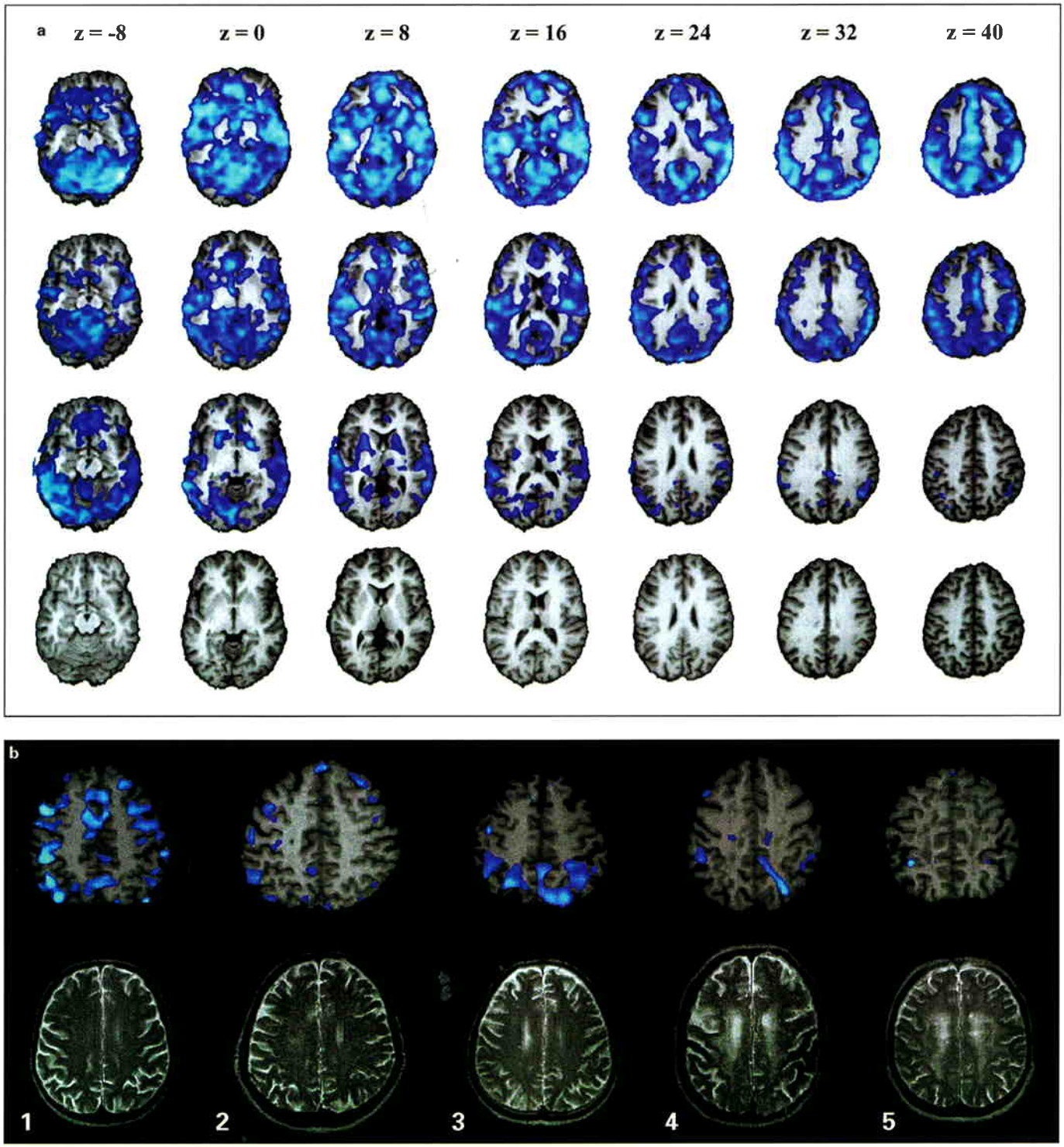

Fig. 1. a Averaged vasoreactivity maps ($z < -5$) acquired as the response to hyperventilation for the different study groups. The z-values reflect the position of the slices in the Talairach coordinate system. 1st row: young controls; 2nd row: elderly controls; 3rd row: patients with cerebral microangiopathy; 4th row: anatomical reference images. **b** Individual vasoreactivity maps of individual patients. A representative axial slice with the fMRI signal decrease (blue) is shown (top row). The corresponding slice in the T_2-weighted sequence displays morphological MR abnormalities in individual patients.

nificant differences between study groups. The normalized and averaged group results were displayed onto a reference 3D dataset (fig. 1a). The strongest effect of hyperventilation – regardless of regional differences – was evident in the group of younger controls, who displayed a significant MR signal decrease in all cortical as well subcortical gray matter compartments. Less extended, although significant, MR signal decreases in response to hyperventilation were observed in elderly subjects. The overall weakest effect of hyperventilation was observed in the patient group. Figure 1b visualizes the individual BOLD signal changes of each individual patient together with the corresponding anatomical scan in the T_2-weighted sequence. A prototypical axial slice was chosen.

Quantitative assessment of the overall MR-signal decrease evaluated the spatial extent of the BOLD signal changes at a certain significance level, i. e. all voxels with a z-score lower than –5: Based on this analysis, young controls showed a significant mean BOLD decrease in 720 ± 130 cm^3 of the overall brain volume. The elderly group showed a significant BOLD signal change in 480 ± 160 cm^3. In contrast, hyperventilation in the patient group was associated with a mean BOLD decrease in only 290 ± 190 cm^3. All differences between groups were significant (young versus elderly controls, $p = 0.04$; young controls versus patients, $p = 0.004$; elderly controls versus patients, $p = 0.05$).

Moreover, the regional intensity, i. e. the magnitude of the MR signal changes was assessed in a ROI analysis of cortical regions in all brain lobes.

This qualitative analysis of the MR signal changes in response to hyperventilation revealed significant regional differences in all groups (fig. 1). The clearest group differences were obtained from the frontal cortices. While patients showed a small BOLD signal intensity change in frontal cortices of –0.62 ± 0.17 %, young and elderly controls were found to have more pronounced BOLD signal decreases: –1.87 ± 0,26 and –2.02 ± 0.4%, respectively. Significant differences were found when comparing young controls and patients in frontal ($p < 0.0001$), parietal ($p = 0.001$) and occipital ($p < 0.0001$) cortices (t test for unpaired samples). However, the temporal and cerebellar cortices did not show significant group differences in the BOLD signal decrease in response to hyperventilation. For the comparison of elderly controls versus patients, significant qualitative BOLD changes were found in frontal ($p = 0.001$) and parietal ($p = 0.017$) cortices. The comparison of the young and elderly control groups yielded only one significant qualitative MR signal change in occipital cortices ($p = 0.03$), all other cortical regions showed a comparable magnitude of the BOLD decrease in response to hyperventilation. Figure 2 displays the regional differences for the selected ROIs in the three study groups.

Correlation to Clinical Data and Structural MR

An interesting relationship became evident when comparing the hyperventilation-induced MR signal decreases in each patient to clinical and morphological data: the degree of global MR signal decrease correlated negatively to the overall severity of structural MR abnormalities, as evaluated by the MR rating score ($r = –0.92$, $p = 0.002$). The resulting MR scores and VR indices are listed in figure 3. No significant relation between the hyperventilation effect and any other clinical parameters was evident.

Discussion

In our study, CR was assessed as the vascular response to hyperventilation measured by means of fMRI BOLD signal changes. The resulting 3D vasoreactivity maps provide strong evidence for altered cerebral hemodynamics in CM. Changes consist of quantitative and qualitative alterations of CR values compared with an age-matched control group, i.e. the spatial extent and the intensity of the MR response showed differences within the study groups. Our findings are in line with recent studies on this topic performed with a variety of measurement methods: i.e. transcranial Doppler, PET, SPECT and NIRS. Moreover, our pilot study shows strong evidence for a regionally differentiated impairment of cerebral autoregulation in the patient group. A strong association between structural MR abnormalities and the degree of CR reductions was evident.

We propose the fMRI hypocapnia protocol as a feasible procedure for characterizing cerebral autoregulation. The hyperventilation task could easily be performed by both healthy controls and CM patients after a short training period. The resulting level of hypocapnia did not statistically differ among the three groups, and hence delivered a comparable challenge for cerebral autoregulation in all controls and patients. Our pilot study included patients with CM to establish the fMRI protocol. Patients showed significantly reduced quantitative CR values in response to the CO_2 challenge, on average 40% less than the corresponding value of age-matched controls and even 60% less than young controls. The observed magnitude of the BOLD signal intensity changes reached mean values between 1.5 and 3.0% in young and elderly controls. In

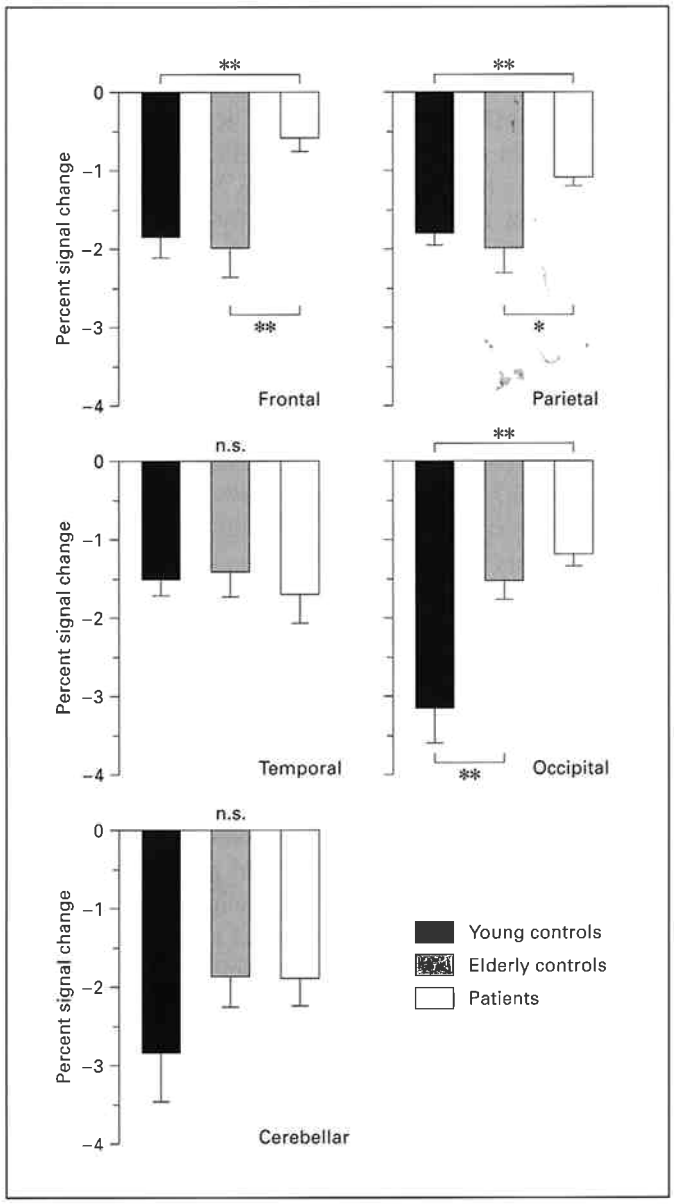

Fig. 2. The magnitude of the MR signal changes in response to hyperventilation: the results and the standard errors for cortical regions in all brain lobes are shown separately for the three study groups. Significant group differences are marked: * $p < 0.05$ and ** $p < 0.001$. Note the small signal changes in frontal cortices in the patient group.

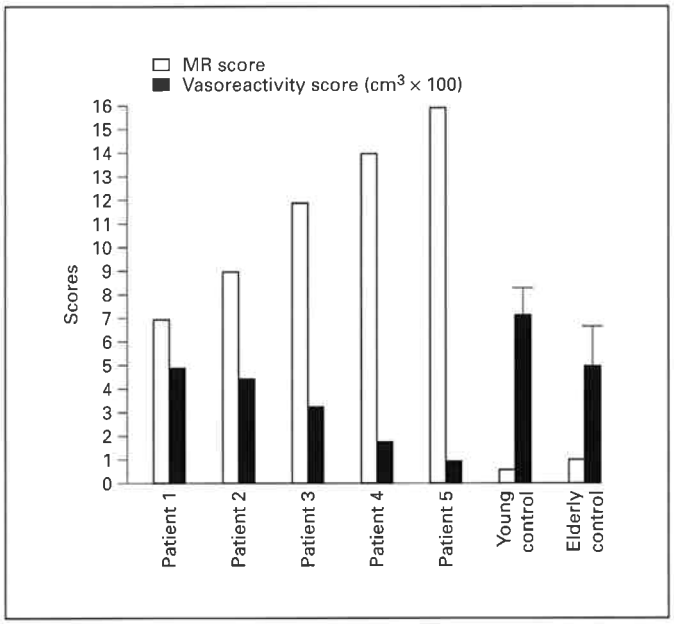

Fig. 3. The degree of structural abnormalities assessed by morphological MR imaging is displayed together with the impairment of cerebral autoregulation as defined by reduced MR BOLD signal changes in response to hyperventilation for each individual patient and the group means and standard deviations of young and elderly controls.

contrast patients showed significantly reduced signal changes of 0.5–2.0%.

Previous autoregulation studies of patients with CM based on various methodologies and protocols have suggested a global impairment of autoregulation. Maeda et al. [11] found a characteristic relation between various types of ischemic cerebrovascular disease and patterns of impaired autoregulation. They found bilateral and global decreases in CR values in patients with multiple lacunar infarctions, while cortical infarctions were associated with ipsilateral impairment of autoregulation. Terborg et al. [12]. reported a reduced vasomotor reactivity as an indicator of the severity of CM in a comparative Doppler and NIRS study. These noninvasive techniques basically express autoregulation in terms of a global vasoreactivity index based on dynamic changes of flow velocities in the middle cerebral artery in response to the CO_2 challenge. PET in contrast can directly measure the cerebral blood volume , the cerebral blood flow and the cerebral metabolic rate of oxygen change of each brain region [9, 14]. Owing to its radiation exposure and lack of wide availability, its application for diagnostic screening in patients is however questionable. Nevertheless, PET and SPECT contributed much to the understanding of dynamic changes in response to a CO_2 or pharmacological challenge. Earlier studies in this field showed that cerebral autoregulation is increasingly impaired with an increasing amount of lacunar infarctions [5]. Moreover, it was reported that white matter abnormalities plus lacunes

result in a more reduced regional cerebral blood flow as compared to structural white matter involvement alone [28]. Much effort has been undertaken to detect the underlying type of dementia, i.e. vascular versus Alzheimer type by means of impaired autoregulation patterns [7, 29, 30]. Our preliminary study shows noninvasively that the severity of structural abnormalities coincides with the quantitative and qualitative alterations of the fMRI-based vasoreactivity in cerebral cortices.

Multiple physiological parameters account for changes in the BOLD signal such as cerebral blood flow, volume and oxidative metabolism as well as in the regional microvascular anatomy [31, 32]. The uniform global stimulus of controlled hypocapnia in our study was thought to best reflect the regional variability of the BOLD signal changes, and thereby allow an estimation of the CR. Very robust CR correlates, as determined by the spatial extent of the BOLD signal decreases, were found in the cerebellar, temporal and occipital cortices of all subjects and patients examined. In healthy subjects, the regional variability of the BOLD response to a global challenge has previously been hypothesized to reflect the regional variability of the capillary and small vessel architecture in addition to the subsequent evolution of changes in the resting state volume [33, 34]. Comparative morphometric studies of the brain demonstrated that the characteristics of the capillary system show a regional variation: i.e. the cerebellar followed by the occipital and parietal cortices have the highest capillary density [35]. The capillary density is closely associated with the regional density of small arterioles, which are known to exhibit – as major resistance vessels – the major hypocapnic flow changes. Regarding the regional magnitude of the BOLD signal intensities, patients with CM showed a drastically reduced frontal signal change, and moreover grossly reduced CR correlates in parietal cortices. How do these findings fit into the pathophysiological models of CM? In patients with CM, the expected scheme of regional BOLD signal changes is definitely determined by lipohyalinosis of the arterioles; this results per se in a decreased cerebral blood flow and coincides with structural abnormalities. They also show a preponderance in certain brain regions: mainly in the deep and subcortical white matter of the frontal and parietal lobes and around the lateral ventricles. Among other factors, the differential regional vasoreactivity detected by BOLD signal changes must be a major factor in determining the differential regional vulnerability of the brain parenchyma in patients with CM. Our hypothesis is supported by earlier work of de Reuck et al. [7], who also found decreased blood flow values mainly in frontal and parietal brain regions of patients with CM. It was suggested that the pathogenesis of CM is variable, depending on the topographic location in the brain. Noteworthy, our fMRI protocol assesses CR values only in the cerebral cortex which is characterized by the highest density of the cerebral microvasculature. Structural MR abnormalities in CM involve essentially the white matter and may evolve as a result of impaired autoregulation.

What are the criteria to assess an impaired CR by means of fMRI BOLD signal changes? In this preliminary study, the quantitative and the qualitative changes of the BOLD signal decrease were most appropriate to identify impaired cerebral autoregulation. In particular, the frontal brain parenchyma exhibited a reduced capacity to react to the CO_2 challenge in patients with CM. The close relation between the degree of morphological abnormalities in patients with CM and impaired autoregulation is intriguing and merits further research. Corresponding observations have been reported from other groups based on different techniques. If a regional decline of CR precedes structural damage in chronic CM, this could be the starting point of a new therapeutic and diagnostic regime during the follow-up of CM.

From previous PET research there is evidence that neuropsychological impairment in CM correlates with the reduction of regional blood flow and glucose utilization [36]. The authors attributed a higher influence of hemodynamic insufficiencies as compared to structural brain abnormalities to evoke cognitive deficits. Future research in this field will have to settle the question whether impaired regional CR patterns are paralleled not only by corresponding structural abnormalities but also by corresponding neuropsychological deficits.

References

1 Fisher CM: Lacunes, small deep cerebral infarcts. Neurology 1965;15:774–784.
2 Hund-Georgiadis M, Ballaschke O, Scheid R, Norris DG, von Cramon DY: Characterization of cerebral microangiopathy using 3 tesla MRI: A correlation with neurological impairment and risk factor profile. J Magn Reson Imaging 2002;15:1–8.
3 Brun A, Fredriksson K, Gustafson L: Pure subcortical arteriosclerotic encephalopathy (Binswanger's disease) a clinicopathological study. Cerebrovasc Dis. 1992;2:87–92.
4 Pantoni L, Garcia JH: Pathogenesis of leukoaraiosis: A review. Stroke 1997;28:652–659.
5 Mochizuki Y, Oishi M, Takasu T: Cerebral blood flow in single and multiple lacunar infarctions. Stroke 1997;28:1458–1460.
6 Reiche W, Weiller C, Weigmann R, Kaiser HJ, Bull U, Scheider R, Ringelstein EB: A comparison of MRT and SPECT findings in patients with cerebral microangiopathy. Nuklearmedizin 1991;30:161–169.
7 De Reuck J, Decoo D, Hasenbroekx MC, et al: Acetazolamide vasoreactivity in vascular dementia: A positron emission tomographic study. Eur Neurol 1999;41:31–36.
8 Tsuda Y, Hartmann A: Changes in hyperfrontality of cerebral blood flow and carbon dioxide reactivity with age. Stroke 1989;20:1667–1673.
9 Bednarczyk EM, Rutherford WF, Leisure GP, et al: Hyperventilation-induced reduction in cerebral blood flow: Assessment by positron emission tomography. Ann Pharmacother 1990;24:456–460.
10 Kastrup A, Dichgans J, Niemeier M, Schabet M: Changes of cerebrovascular CO_2 reactivity during normal aging. Stroke 1998;29:1311–1314.
11 Maeda H, Matsumoto M, Handa N, Hougaku H, Ogawa S, Itoh T: Reactivity of cerebral blood flow to carbon dioxide in various types of ischemic cerebrovascular disease: Evaluation by the transcranial Doppler method. Stroke 1993;24:670–675.
12 Terborg C, Gora F, Weiller C, Rother J: Reduced vasomotor reactivity in cerebral microangiopathy: A study with near-infrared spectroscopy and transcranial Doppler sonography. Stroke 2000;31:924–929.
13 Posse S, Dager SR, Richards TL, et al: In vivo measurement of regional brain metabolic response to hyperventilation using magnetic resonance: Proton echo planar spectroscopic imaging (PEPSI). Magn Reson Med 1997;37:858–865.
14 Rostrup E, Law I, Blinkenberg M, et al: Regional differences in the CBF and BOLD responses to hypercapnia: A combined PET and fMRI study. Neuroimage 2000;11:87–97.
15 Naganawa S, Norris DG, Zysset S, Mildner T: Regional differences of fMR signal changes induced by hyperventilation: Comparison between SE-Epi and GE-Epi at 3T. J Magn Reson Imaging 2002;15:23–30.
16 Toft PB, Leth H, Lou HC, Pryds O, Peitersen B, Henriksen O: Local vascular CO_2 reactivity in the infant brain assessed by functional MRI. Pediatr Radiol 1995;25:420–424.
17 Hund-Georgiadis M, Norris DG, Guthke T, von Cramon DY: Characterization of cerebral small vessel disease by proton spectroscopy and morphological magnetic resonance. Cerebrovasc Dis 2002;12:82–90.
18 Hantson L, De Weerdt W, De Keyser J, Diener HC, Franke C: Palm Ret. The European Stroke Scale. Stroke 1994;25:2215–2219.
19 Norris DG: Reduced power multislice MDEFT imaging. J Magn Reson Imaging 2000;11:445–451.
20 Lohmann G, Mueller K, Bosch V, Mentzel H, Hessler S, Chen L, Zysset S, von Cramon DY: LIPSIA – A new software system for the evaluation of functional magnetic resonance images of the human brain. Comput Med Imaging Graph 2001;25:449–457.
21 Ugurbil K, Garwood M, Ellermann J, et al: Imaging at high magnetic fields: Initial experiences at 4 T. Magn Reson Q 1993;9:259–277.
22 Talairach J, Tournoux P: Co-Planar Stereotaxic Atlas of Human Brain. New York, Thieme, 1988.
23 Friston KJ: Statistical parametric maps in functional imaging: A general linear approach. Hum Brain Mapp 1994;2:189–210.
24 Friston KJ, Holmes AP, Poline J-B, Grasby BJ, Williams CR, Frackowiak RSJ, Turner R: Analysis of fMRI time-series revisited. NeuroImage 1995;2:45–53.
25 Worsley KJ, Friston, KJ: Analysis of fMRI time-series revisited – again. NeuroImage 1995;2:359–365.
26 Zarahn E, Aguirre GK, D'Esposito M: Empirical analyses of BOLD fMRI statistics. NeuroImage 1997;5:179–197.
27 Bosch V: Statistical analysis of multi-subject fMRI data: The assessment of focal activations. J Magn Reson Imaging 2000;11:61–64.
28 Oishi M, Mochizuki Y: Cerebrovascular acetazolamide reactivity and platelet function in asymptomatic cerebral thrombosis. J Neurol Sci 1999;166:81–84.
29 Ries D, Horrn R, Hillekamp J, Honisch C, Konig M, Solymosi L: Differentiation of multiinfarct and Alzheimer dementia by intracranial hemodynamic parameters. Stroke1993;24:228–235.
30 Markos A, Egido JA, Barquero M, Fernandez C, de Seijas EV: Full range of vasodilatation tested by transcranial Doppler in the differential diagnosis of vascular and Alzheimer types of dementia. Cerebrovasc Dis 1997;7:14–18.
31 Kastrup A, Kruger G, Glover GH, Neumann-Haefelin T, Moseley ME: Regional variability of cerebral blood oxygenation response to hypercapnia. Neuroimage 1999;10:675–681.
32 Hoge RD, Atkinson J, Gill B, Crelie GR, Marrett S, Pike GB: Investigation of BOLD signal dependence on cerebral blood flow and oxygen consumption: The deoxyhemoglobin dilution model. Magn Reson Med 1999;42:849–863.
33 Boxerman JL, Bandettini PA, Kwong KK, et al: The intravascular contribution to fMRI signal change: Monte Carlo modeling and diffusion-weighted studies in vivo. Magn Reson Med 1995;34:4–10.
34 Leenders KL, Perani D, Lammertsma AA, Heather JD, Buckingham P, Healy MJ, Gibbs JM, Wise RJ, Hatazawa J, Herold S: Cerebral blood flow, blood volume and oxygen utilization: Normal values and effect of age. Brain 1990;113:27–47.
35 Lierse W: Die Kapillardichte im Wirbeltiergehirn. Acta Anat 1963;54:1–31.
36 Sabri O, Ringelstein EB, Hellwig D, Schneider R, Schreckenberger M, Kaiser HJ, Mull M, Buell U: Neuropsychological impairment correlates with hypoperfusion and hypometabolism but not with severity of white matter lesions on MRI in patients with cerebral microangiopathy. Stroke 1999;30:556–566.